BJP British Journal of Pharmacology

DOI:10.1111/bph.12251
www.brjpharmacol.org

RESEARCH PAPER

Spinal actions of ω-conotoxins, CVID, MVIIA and related peptides in a rat neuropathic pain model

A Jayamanne[1], H J Jeong[1], C I Schroeder[2], R J Lewis[2], M J Christie[3] and C W Vaughan[1]

[1]*Pain Management Research Institute, Kolling Institute, Northern Clinical School, The University of Sydney, Sydney, NSW, Australia,* [2]*Institute for Molecular Bioscience, University of Queensland, Brisbane, NSW, Australia, and* [3]*Discipline of Pharmacology, The University of Sydney, Sydney, NSW, Australia*

Correspondence
Professor MacDonald J. Christie, Pharmacology, D06, University of Sydney, Sydney, NSW 2006, Australia. E-mail: mac.christie@sydney.edu.au

Keywords
pain; neuropathic; calcium channel; conotoxin; synaptic neurotransmission

Received
2 December 2012
Revised
1 May 2013
Accepted
16 May 2013

BACKGROUND AND PURPOSE

Antagonists of the N-type voltage gated calcium channel (VGCC), $Ca_v2.2$, have a potentially important role in the treatment of chronic neuropathic pain. ω-conotoxins, such MVIIA and CVID are effective in neuropathic pain models. CVID is reported to have a greater therapeutic index than MVIIA in neuropathic pain models, and it has been suggested that this is due to faster reversibility of binding, but it is not known whether this can be improved further.

EXPERIMENTAL APPROACH

We examined the potency of CVID, MVIIA and two intermediate hybrids ([K10R]CVID and [R10K]MVIIA) to reverse signs of neuropathic pain in a rat nerve ligation model in parallel with production of side effects. We also examined the potency and reversibility to inhibit primary afferent synaptic neurotransmission in rat spinal cord slices.

KEY RESULTS

All ω-conotoxins produced dose-dependent reduction in mechanical allodynia. They also produced side effects on the rotarod test and in a visual side-effect score. CVID displayed a marginally better therapeutic index than MVIIA. The hybrids had a lesser effect in the rotarod test than either of their parent peptides. Finally, the conotoxins all presynaptically inhibited excitatory synaptic neurotransmission into the dorsal horn and displayed recovery that was largely dependent upon the magnitude of inhibition and not the conotoxin type.

CONCLUSIONS AND IMPLICATIONS

These findings indicate that CVID provides only a marginal improvement over MVIIA in a preclinical model of neuropathic pain, which appears to be unrelated to reversibility from binding. Hybrids of these conotoxins might provide viable alternative treatments.

Introduction

Neuropathic pain caused by damage to peripheral nerves, the spinal cord or brain by physical trauma and disease is a debilitating pain state. This is characterized by a persistent abnormal pain syndrome that includes allodynia, spontaneous pain, dysesthesia plus a range of psychosocial problems (Jensen *et al.*, 2011). Chronic neuropathic pain is problematic because currently recommended pharmacological treatments have limited or variable efficacy, and are often associated with intolerable side effects (Dworkin *et al.*, 2010).

Voltage gated calcium channel (VGCC) antagonists represent a potentially important class of analgesic agents for neuropathic pain (for review, see McGivern, 2006; Adams *et al.*, 2012). Of particular interest are the N-type VGCCs, $Ca_v2.2$ (Alexander *et al.*, 2011), localized on nociceptive

primary afferent neurons and their terminals within the superficial dorsal horn (Westenbroek *et al.*, 1992; Snutch, 2005). A number of structurally related ω-conotoxins, including MVIIA, GVIA and CVID, have been extracted from the genus *Conus* (cone snails) that selectively inhibit $Ca_v2.2$ VGCCs (Adams *et al.*, 2012; Lewis *et al.*, 2012). Synthetic derivatives of MVIIA (Prialt, SNX-111, ziconotide) and CVID (AM336) have shown clinical potential but must be delivered spinally to remain safe (McGivern, 2006). Preclinical studies have shown that intrathecally delivered MVIIA and CVID reduce the allodynia associated with rodent models of neuropathic pain (Chaplan *et al.*, 1994; Bowersox *et al.*, 1996; Scott *et al.*, 2002; Blake *et al.*, 2005; Souza *et al.*, 2008; Hama and Sagen, 2009; Berecki *et al.*, 2010; Ogawa *et al.*, 2011; Morimoto *et al.*, 2012). While the spinal analgesic actions of both MVIIA and CVID are associated with a number of side effects, CVID displays a much greater therapeutic index (TI) than MVIIA (Wright *et al.*, 2000; Scott *et al.*, 2002; Smith *et al.*, 2002).

The improved TI of CVID versus MVIIA could be due to a number of factors, including greater selectivity of CVID for $Ca_v2.2$ versus $Ca_v2.1$ (P/Q type) calcium channels, and differences in their biophysical properties, or pharmacokinetic profiles (Lewis *et al.*, 2000; Mould *et al.*, 2004; McGivern, 2006). One difference between these conotoxins is that the inhibition of VGCC currents in isolated neurons produced by CVID is more reversible after washout than for MVIIA, and this is due largely to one residue of the peptide sequence (Mould *et al.*, 2004). Mutation of position 10 of the peptide CVID ([K10R]CVID) impairs the reversibility of VGCC inhibition, while mutation in MVIIA ([R10K]MVIIA) increases the reversibility (Adams *et al.*, 2003; Mould *et al.*, 2004).

In the present study, we compared the analgesic and side effects produced by intrathecal administration of the ω-conotoxins CVID, MVIIA and the hybrids, [K10R]CVID and [R10K]MVIIA, in a rat model of neuropathic pain to determine whether or not substitution of this residue altered the TI of either CVID or MVIIA. *In vitro* slice studies have shown that $Ca_v2.2$ VGCC blockers MVIIA and CVID reduce primary afferent evoked EPSCs in superficial dorsal horn neurons via a presynaptic mechanism (Rycroft *et al.*, 2007; Motin and Adams, 2008). We also therefore compared their effects on primary afferent evoked synaptic transmission into the superficial dorsal horn to determine whether their pain-relieving actions were reflected in their spinal cellular actions.

Methods

Experiments were carried out on 2- to 3-week-old (electrophysiology) and 8- to 10-week-old (behaviour) Sprague-Dawley rats, following the guidelines of the 'NH&MRC Code of Practice for the Care and Use of Animals in Research in Australia' and with the approval of the Royal North Shore Hospital Animal Care and Ethics Committee. Animals were housed under a 12:12-h light/dark cycle, with environmental enrichment and free access to water and standard rat chow. Eight- to ten-week-old animals were housed in groups of three; 2- to 3-week-old animals were housed with their littermates and mother.

Reagents

The ω-conotoxins CVID, MVIIA, [K10R]-CVID and [R10K]-MVIIA were synthesized as described previously (Adams *et al.*, 2003). 6-cyano-7-nitroquinoxaline-2,3-dione (CNQX), dl-(-)-2-amino-5-phosphonopentanoic acid (AP5) and n-ethyllidocaine bromide (QX314) were from Ascent Scientific (Bristol, UK); picrotoxin, strychnine hydrochloride and all other reagents were from Sigma (Sydney, Australia).

Behavioural experiments

Behavioural experiments were carried out on adult male rats, as previously (Ekberg *et al.*, 2006; Vuong *et al.*, 2008). All animals were allowed to acclimatize to their holding cages for 2–3 days before any procedures were carried out. All surgical procedures were carried out under isoflurane (1–3% in O_2) anaesthesia. Rats underwent partial ligation of the sciatic nerve (PNL) (Seltzer *et al.*, 1990). The left sciatic nerve was exposed at mid-thigh level approximately 3 mm proximal to the trifurcation of the sciatic nerve at the popliteal fossa. A 4-0 silk suture was inserted into the nerve to tightly ligate the dorsal 1/3–1/2 of the nerve trunk. The muscle (4-0) and skin (3-0) were closed with silk sutures. Nine days after PNL surgery, chronic polyethylene lumbar intrathecal catheters were inserted between vertebrae L5 and L6, advanced 3 cm rostrally and exteriorized via the occipital region.

To assess mechanical allodynia, the mechanical paw withdrawal threshold (PWT) was measured with a series of von Frey hairs (range 0.4–15 g) and calculated using the up-down paradigm (Chaplan *et al.*, 1994). A plantar tester (Ugo Basile, Comerio, Italy) was used to measure thermal pain. Rats were placed in Perspex enclosures (15 × 15 × 18 cm). Focal IR heat was applied through the glass bottom of the enclosure to the left hind paw, and the time for the rat to respond by moving its paw away from the noxious heat source was recorded (thermal paw withdrawal latency, PWL). Rats were given 10–15 min to acclimate to each of these devices before measurements were taken. To assess side effects, motor performance was measured as the duration for which the animal could maintain balance on the rotating drum of a rotarod device (Ugo Basile), with a maximal cut-off time of 300 s. A qualitative scoring of side effects was also used (Scott *et al.*, 2002). Over the first 2 h after drug injection, animals were scored as follows: 0 if no side effects, 1 if mild side effects (occasional spontaneous tail twitching, lower back hunching or piloerection), 2 if moderate side effects (frequent tail flicks or occasional writhing of the tail, and spontaneous hind limb twitching accompanied by ataxia, and frequent urination), 3 if severe side effects (marked tail writhing occurred along with frequent hind limb twitching or hind limb splaying and an inability to walk normally).

All procedures were carried out in the light cycle. Animals were acclimatized to the testing devices before and 7 days after PNL surgery, then before intrathecal catheter placement. Solutions of all agents were made up just prior to administration. All agents were made up in a vehicle solution of normal saline and injected intrathecally in a total volume of 20 μL, followed by a 15-μL flush of normal saline. Each animal underwent one drug injection experiment. On this day, testing was carried out twice out over a 30-min period before, then at set time points over a 4- to 6-h period following intrathecal drug injection. The experimenter was blind to

the drug being tested. Afterwards, catheter placement was confirmed by the occurrence of rapid, bilateral hind limb paralysis following intrathecal injection of lignocaine (2%). Conotoxins were injected at doses between 0.01 and 0.3 nmol, which corresponded approximately to 0.1–3 $\mu g \cdot kg^{-1}$. The highest dose of conotoxin tested was that at which a maximal side-effect score was observed in two or more animals.

Electrophysiological experiments

Electrophysiological experiments were carried, out as described previously (Jeong *et al.*, 2010). Animals were deeply anaesthetized with isoflurane and decapitated. The spinal cord was exposed, the dura was incised, and the spinal column quickly removed and placed in ice-cold artificial CSF (ACSF) of composition: (mM): NaCl, 126; KCl, 2.5; NaH_2PO_4, 1.4; $MgCl_2$, 1.2; $CaCl_2$, 2.4; glucose, 11; $NaHCO_3$, 25. Transverse (300 µm) slices of the lumbar spinal cord (L4–6) were obtained using a vibratome (VT1000S: Leica, Nussloch, Germany) and maintained at 32–34°C in a submerged chamber containing ACSF equilibrated with 95% O_2 and 5% CO_2. Individual slices were transferred to a slice chamber (volume 0.5 mL) and superfused continuously (2.2–2.5 $mL \cdot min^{-1}$) with ACSF at 32–34°C using an inline temperature controller.

Superficial dorsal horn neurons located throughout lamina II were visualized using IR Dodt-tube or Nomarski optics on an upright microscope (Olympus BX50, Olympus, Sydney, Australia) and whole-cell voltage clamp recordings (holding potential 65 mV, liquid junction potential corrected) were made using an Axopatch 200B (Molecular Devices, Sunnyvale, CA, USA). The internal solution contained (mM): CsCl 140, HEPES 10, EGTA 0.2, $MgCl_2$ 1, QX314 3, MgATP 2 and NaGTP 0.3 (pH 7.3 and osmolality 280–285 $mosmol \cdot L^{-1}$). Series resistance (<25 MΩ) was compensated by 80% and continuously monitored during experiments. Electrically evoked EPSCs were elicited in neurons via a glass unipolar stimulating electrode placed on the dorsal root (once every 12 s, intensity 2–25 V, 0.1–0.3 ms) in the presence of the $GABA_A$ channel blocker picrotoxin (100 µM), the glycine receptor antagonist strychnine (3 µM) and the NMDA receptor antagonist AP5 (25 µM). The evoked EPSCs were classified as monosynaptic if the initial EPSC displayed little variability in its onset (Berry and Pentreath, 1976). Stock solutions of all conotoxins were diluted (1:1000–10 000) to working concentrations in ACSF immediately before use and applied by superfusion to the slice chamber.

Analysis

For behavioural experiments, comparisons of drug effects over time were made using two-way ANOVAs, with time and drug treatment as a within- and between-subjects factors (Prism, GraphPad Software, La Jolla, CA, USA). When two-way ANOVAs were significant post-hoc comparisons between drug treatment groups and vehicle at individual time points were made using the Bonferroni adjustment for multiple comparisons. Dose response profiles in behavioural experiments were calculated as an average over the 1- and 2-h time points post-drug injection (time at which maximal effects were observed) and transformed into their maximum possible effect (%MPE): mechanical PWT = (drug – pre-drug)/(15 – pre-drug); rotarod = (pre-drug – drug)/(pre-drug); side effect = (drug)/3. The %MPE values were compared using one-way ANOVAs (or Kruskal–Wallis non-parametric test for side-effect scores) and when significant, post-hoc comparisons between drug treatment groups and vehicle were made using Dunnett's (or Dunn's) adjustment for multiple comparisons. The ED_{50}s were calculated for %MPE data using a sigmoidal fit with a variable slope (Prism).

For electrophysiological experiments, recordings were filtered (2 kHz low-pass filter) and sampled (10 kHz) for online and offline analysis using AxographX (Axograph Scientific, Sydney, Australia). Evoked EPSC amplitude was measured as the difference between the peak of the EPSC and a 2-ms baseline period preceding the stimulus artefact, and values were calculated as the mean over a 2 min period. The drug effect was calculated as follows: drug inhibition (%) = (pre-drug – drug)/(pre-drug), recovery following 20 min drug washout (%) = (post-drug – drug)/(pre-drug – drug). Statistical assessment of individual drug effects was made using paired *t*-tests. Differences were considered significant when $P < 0.05$ and all numerical data are expressed as mean ± SEM.

Results

Effect of intrathecal conotoxins in a neuropathic pain model

In animals that underwent partial sciatic nerve ligation and chronic implantation with lumbar intrathecal catheters, the mechanical PWT was 14.9 ± 0.1 g prior to PNL surgery, 0.7 ± 0.1 g at 9 days post-PNL surgery (prior to intrathecal catheterization) and 0.6 ± 0.6 g at 14 days post-PNL surgery (4 days after intrathecal catheterization, $n = 65$). The thermal PWL was 7.7 ± 0.5, 6.8 ± 0.8 and 6.2 ± 0.4 s, while the rotarod latency was 143 ± 9, 103 ± 11 and 86 ± 8 s at the same time points.

The intrathecal actions of the conotoxins of a 0.1 nmol dose (~1 $\mu g \cdot kg^{-1}$) of CVID and MVIIA, plus the hybrids [K10R]CVID and [R10K]MVIIA were first examined at 14 days post-PNL surgery (4 days post-intrathecal catherization). The effect of CVID, [K10R]CVID, [R10K]MVIIA, MVIIA and vehicle on mechanical PWT differed significantly over time [$P < 0.0001$, $F(20, 205) = 8.1$]. CVID ($n = 11$) produced a reversible increase in mechanical PWT that was significantly greater than vehicle ($n = 17$) at 1–4 h post-injection (Figure 1A, $P < 0.01$–0.001). MVIIA ($n = 6$) and [R10K]MVIIA ($n = 6$) produced the greatest increase in mechanical PWT, and this was significantly greater than vehicle at 1–6 h post-injection (Figure 1A, $P < 0.001$–0.0001, MVIIA and [R10K]MVIIA). [K10R]CVID ($n = 6$) produced a lesser increase in mechanical PWT that was only significantly greater than vehicle at 2 h post-injection (Figure 1A, $P < 0.01$). It might also be noted that while the increase in mechanical PWT produced by CVID and [K10R]CVID returned to pre-injection levels by 4–6 h, the increase in mechanical PWT produced by MVIIA and [R10K]MVIIA remained above pre-injections at 6 h (Figure 1A).

The effect of CVID, [K10R]CVID, [R10K]MVIIA, MVIIA (0.1 nmol) and vehicle on thermal PWL differed significantly

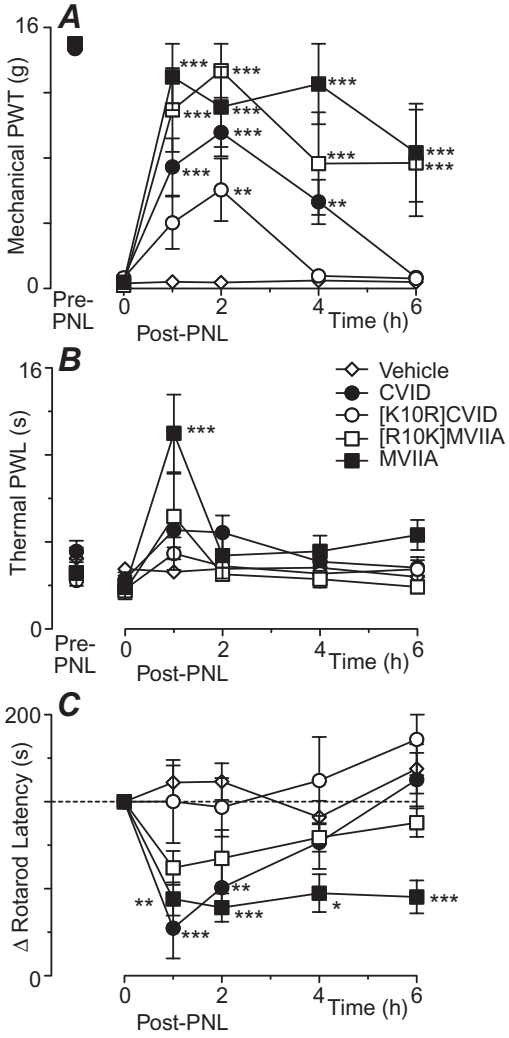

Figure 1

Time course of action of conotoxins in a neuropathic pain model. Time plots of the effect of CVID, [K10R]CVID, [R10K]MVIIA, MVIIA (0.1 nmol) or vehicle on (A) mechanical PWT, (B) thermal PWL, and (C) rotarod latency. Animals received an intrathecal injection of one of the conotoxins or a matched vehicle at time 0 h, 14 days after partial nerve ligation (Post-PNL). Data are also shown prior to PNL surgery (Pre-PNL). *, ** and *** denotes $P < 0.05$, 0.01 and 0.001 compared with vehicle at the corresponding time point. Data for rotarod latency are shown as the difference to that at time 0 prior the drug injection.

over time ($P < 0.0001$, $F(20, 175) = 3.1$). MVIIA ($n = 6$) produced an increase in thermal PWL that was significantly greater than vehicle ($n = 11$) only at 1 h post-injection (Figure 1B, $P < 0.0001$, MVIIA and vehicle). CVID ($n = 11$), [K10R]CVID ($n = 6$) and [R10K]MVIIA ($n = 6$) did not produce an increase in thermal PWL relative to vehicle (Figure 1B, $P > 0.05$, CVID, [K10R]CVID and [R10K]MVIIA).

The effect of CVID, [K10R]CVID, [R10K]MVIIA, MVIIA (0.1 nmol) and vehicle on rotarod latency differed significantly over time [$P < 0.0001$, $F(16, 124) = 3.8$]. MVIIA ($n = 6$) produced a sustained decrease in rotarod latency that was significantly greater than vehicle ($n = 12$) at 1–6 h post-injection (Figure 1C, $P < 0.05$–0.001, MVIIA and vehicle). CVID ($n = 6$) produced a reversible decrease in rotarod latency that was significantly greater than vehicle ($n = 6$) at 1–2 h post-injection (Figure 1C, $P < 0.01$–0.0001). [K10R]CVID ($n = 6$) and [R10K]MVIIA ($n = 6$) did not produce a significant change in rotarod latency relative to vehicle (Figure 1C, $P > 0.05$).

Conotoxins produce dose-dependent analgesia and side effects

We next examined the dose-response profiles of the conotoxins. The net change in mechanical PWT and thermal PWL produced by vehicle and the various doses of CVID, [K10R]CVID, [R10K]MVIIA and MVIIA differed ($P < 0.0001$, $P = 0.04$, $n = 5$–17). CVID produced a net increase in mechanical PWT that was significantly greater than vehicle only at the 0.1–0.3 nmol doses (Figure 2A, $P < 0.001$). [K10R]CVID, [R10K]MVIIA and MVIIA produced a net increase in mechanical PWT that was significantly greater than vehicle at the highest doses tested (Figure 2A, $P < 0.001$ at 0.3, 0.1 and 0.1 nmol). By contrast, CVID, [K10R]CVID, [R10K]MVIIA did not produce a change in thermal PWL significantly different to vehicle ($P > 0.05$), while MVIIA produced a net increase in thermal PWL significantly greater than vehicle at the 0.1 nmol dose ($P < 0.01$, data not shown).

The decrease in rotarod latency and the side-effect score produced by vehicle and the various doses of CVID, [K10R]CVID, [R10K]MVIIA and MVIIA differed significantly ($P < 0.0001$). CVID (0.1, 0.3 nmol) and MVIIA (0.1 nmol) produced a decrease in rotarod latency that was significantly greater than vehicle only at the higher doses (Figure 2B, $P < 0.001$). [K10R]CVID did not produce a significant change in rotarod latency compared with vehicle (Figure 2B, $P > 0.05$). [R10K]MVIIA produced a decrease in rotarod latency that was significantly greater than vehicle only at the 0.1 nmol dose (Figure 2B, $P < 0.05$). The side-effect score was significantly different to vehicle at the higher doses of CVID (0.1, 0.3 nmol), [K10R]CVID (0.3 nmol), [R10K]MVIIA (0.1 nmol) and MVIIA (0.03, 0.1 nmol) (Figure 2C, $P < 0.05$–0.001).

The TI for CVID and MVIIA, calculated as the ratio of the ED_{50}s for the rotarod and side-effect score relative to mechanical PWT, was marginally greater for CVID (1.8, 2.4) than that for MVIIA (1.0, 0.7) (Table 1). Dose-response curves could not be fit to all of the data for the hybrids, so we compared the magnitude of the effect of all conotoxins on mechanical PWT to that for the rotarod and side-effect score, for doses at which there was a significant increase in mechanical PWT (Figure 2D, E). The hybrids [K10R]CVID and [R10K]MVIIA, but not their parent conotoxins CVID and MVIIA, had a lesser effect on rotarod performance compared with mechanical PWT (Figure 2D). All of the conotoxins had a similar effect on the side-effect score compared with mechanical PWT (Figure 2E).

Effect of CVID, MVIIA and hybrids on synaptic transmission into superficial dorsal horn

We next examined the effect of CVID on monosynaptic afferent-evoked synaptic transmission. Electrical stimulation of the dorsal root in the presence of strychnine (3 μM) and

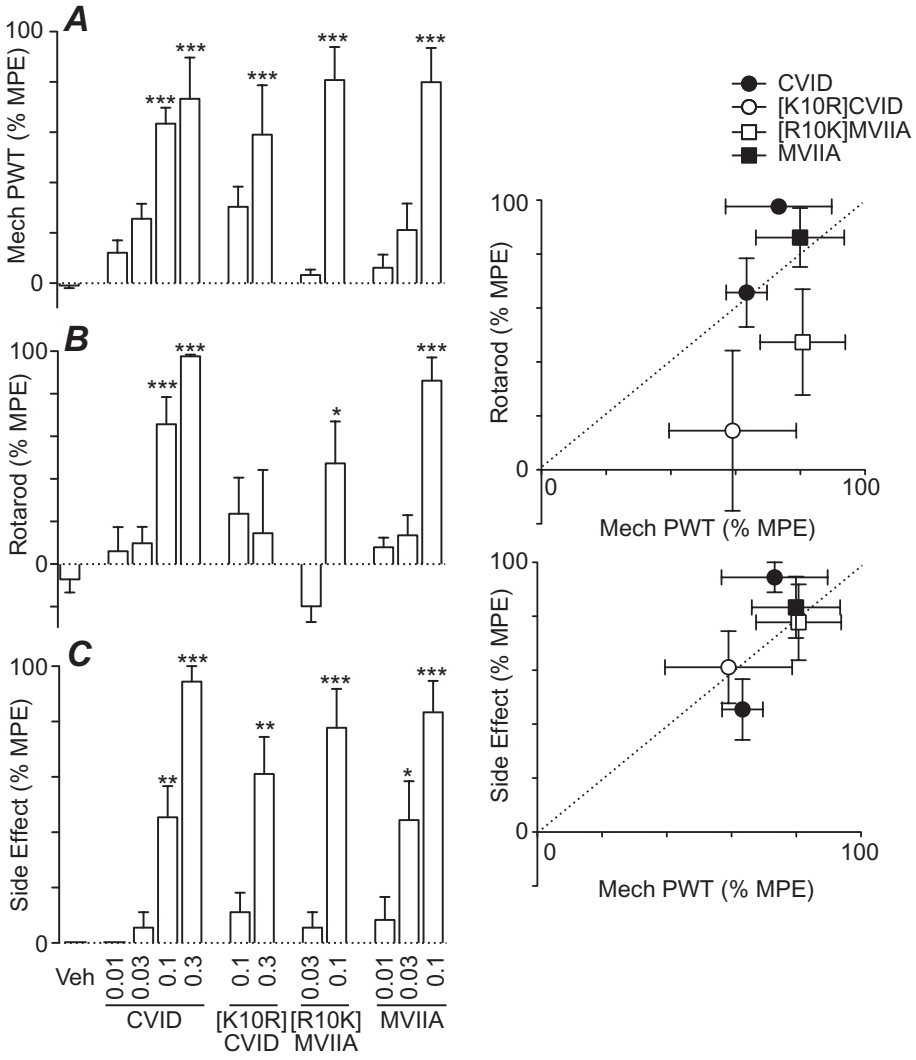

Figure 2

Conotoxins have dose-dependent effects in a neuropathic pain model. Bar charts of the net effect of intrathecal injection of CVID, [K10R]CVID, [R10K]MVIIA, MVIIA and matched vehicle on (A) mechanical PWT, (B) rotarod latency and (C) side-effect score. Plots of the net effect on (D) rotarod latency and (E) side-effects score versus mechanical PWT, for dose in which there is significant effect on mechanical PWT. The net effect was measured as the average over 1–2 h post-drug injection as a percentage of the %MPE. *, ** and *** $P < 0.05$, 0.01 and 0.0001 compared with vehicle. The dotted lines in (D,E) indicate where there was an equal effect on both behavioural assays.

Table 1

Potency and therapeutic index CVID and MVIIA

	CVID		MVIIA	
	ED_{50}	TI	ED_{50}	TI
Mechanical PWT	0.04 (0.02–0.10)		0.06 (0.04–0.08)	
Rotarod	0.08 (0.05–0.12)	1.8	0.06 (0.04–0.08)	1.0
Side-Effect Score	0.11 (0.06–0.19)	2.4	0.04 (0.02–0.06)	0.7

ED_{50} in nmol, shown as mean (95% confidence interval). The TI was calculated as the ratio of the ED_{50} for mechanical PWT : rotarod, and mechanical PWT : visual side-effect score.

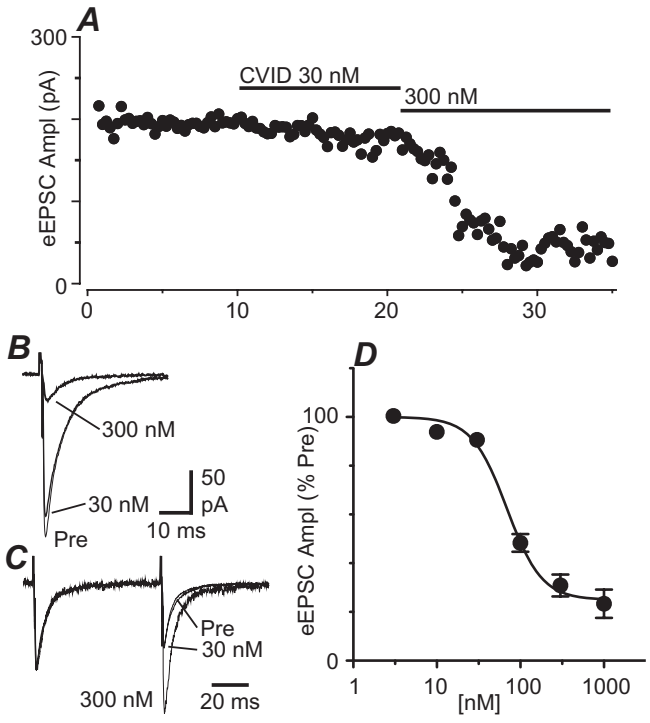

Figure 3

CVID produces concentration-dependent presynaptic inhibition of evoked EPSCs in superficial dorsal horn. (A) Time plot of the amplitude of dorsal root evoked EPSCs in a lamina II neuron during superfusion of CVID 30 nM, then 300 nM. (B) Averaged traces of evoked EPSCs before (pre) and during application 30 and 300 nM CVID. (C) Averaged evoked EPSCs in response to identical paired stimuli (interstimulus interval 70 ms) before (pre) and during 30 and 300 nM CVID, with EPSC1 normalized to demonstrate relative facilitation of EPSC2 during superfusion of CVID. (D) Concentration response curve for the inhibition of evoked EPSC amplitude by CVID, with a logistic function fitted to determine the EC_{50}. In (D), data are shown as the evoked EPSC amplitude in the presence of CVID as a percentage of the pre-CVID value.

picrotoxin (100 μM) produced evoked EPSCs in neurons throughout lamina II of the lumbar dorsal horn that were abolished by the non-NMDA antagonist CNQX (5 μM, $n = 4$). Superfusion of CVID produced a decrease in the amplitude of evoked EPSCs (Figure 3A, B). The inhibition of the amplitude of evoked EPSCs produced by CVID was concentration-dependent, with an EC_{50} of 69 nM (95% confidence interval = 53–90 nM) and a hill slope of 2.1 ± 0.5 (Figure 3A, B, D, n = 3–15). When paired EPSCs were evoked at an interstimulus interval of 70 ms in these neurons, paired pulse depression was observed (paired pulse ratio = 0.39 ± 0.10, range = 0.06–0.70, $n = 9$) (Figure 3C). In the presence of CVID (100–1000 nM), the paired pulse ratio was increased to 150 ± 16 % of the pre-CVID level ($P = 0.01$). The increase in paired pulse ratio produced by CVID had an EC_{50} of 102 nM (95% confidence interval = 15–354 nM).

We also examined the actions of [K10R]CVID, [R10K]MVIIA and MVIIA at a concentration of 100 nM that was just above the EC_{50} concentration for CVID. Superfusion of 100 nM [K10R]CVID ($n = 5$), [R10K]MVIIA ($n = 5$) and MVIIA ($n = 6$) all produced a decrease in the amplitude of evoked EPSCs (Figure 4A–D, $P = 0.0009$, 0.02, 0.0009). The inhibition produced by [R10K]MVIIA was less than that produced by CVID, [K10R]CVID and MVIIA ($P < 0.01$).

It has previously been reported that conotoxins vary in their rate of recovery from binding. We examined recovery of EPSC inhibition in neurons in which only one conotoxin was applied for 10 min at a 100-nM concentration. Following 20 min washout, the amplitude of evoked EPSCs recovered to the pre-drug level for [R10K]MVIIA ($P = 0.6$, $n = 5$) but not for CVID ($P = 0.0002$, $n = 8$), [K10R]CVID (0.006, $n = 5$) and MVIIA (0.001, $n = 6$) (Figure 5C). In these experiments, however, the recovery of evoked EPSCs was highly variable following washout of each of the conotoxins (Figure 5A–C). The recovery from inhibition was inversely related to the inhibition during drug application for CVID, [K10R]CVID, [R10K]MVIIA and MVIIA (Figure 5D). The slope of recovery versus inhibition plots for the different conotoxins were not significantly different ($P = 0.5$, $F(4, 38) = 0.87$, pooled slope = –2.5 ± 0.3).

Discussion

In the present study, it has been demonstrated that the conotoxins CVID, MVIIA and two intermediate hybrids, [K10R]CVID and [R10K]MVIIA, reduce the allodynia-like pain behaviour associated with a nerve injury model of neuropathic pain. CVID displayed a marginally better TI than MVIIA. In addition, the hybrids had a relatively lesser effect on motor performance, but displayed other side-effects that were similar to CVID and MVIIA. The analgesic actions of the different conotoxins were likely to be mediated by a similar presynaptic inhibition of excitatory transmission into the superficial dorsal horn.

In the present study, it was observed that intrathecal delivery of the conotoxins CVID and MVIIA produced an increase in mechanical PWT in animals which had undergone partial ligation of the sciatic nerve, which approached the levels prior to nerve ligation. This indicates that the conotoxins have an anti-allodynic effect in this neuropathic pain model. The potency and efficacy of CVID and MVIIA were similar to that observed in prior studies that have examined the effects of the conotoxins in neuropathic and inflammatory pain models (Malmberg and Yaksh, 1995; Scott *et al.*, 2002; Smith *et al.*, 2002). It was also observed that MVIIA, but not CVID and the hybrid conotoxins, transiently increased thermal PWL to values above the pre-PNL level, indicating that MVIIA produced thermal hypoalgesia. The weak effect of these conotoxins on thermal pain is consistent with the lack of effect of MVIIA and CVID on hot-plate latency in a neuropathic pain model (Scott *et al.*, 2002). It might be noted, however, that MVIIA reduces thermal hyperalgesia in the chronic constriction injury model but not in the spinal nerve ligation model (Yamamoto and Sakashita, 1998). These findings indicate that conotoxins may be particularly effective in targeting mechanical allodynia in neuropathic pain models.

The reduction in allodynia produced by the conotoxins was associated with side effects that included reduced motor performance on the rotarod, plus visually scored behaviours ranging from piloerection and twitching to seizures at the

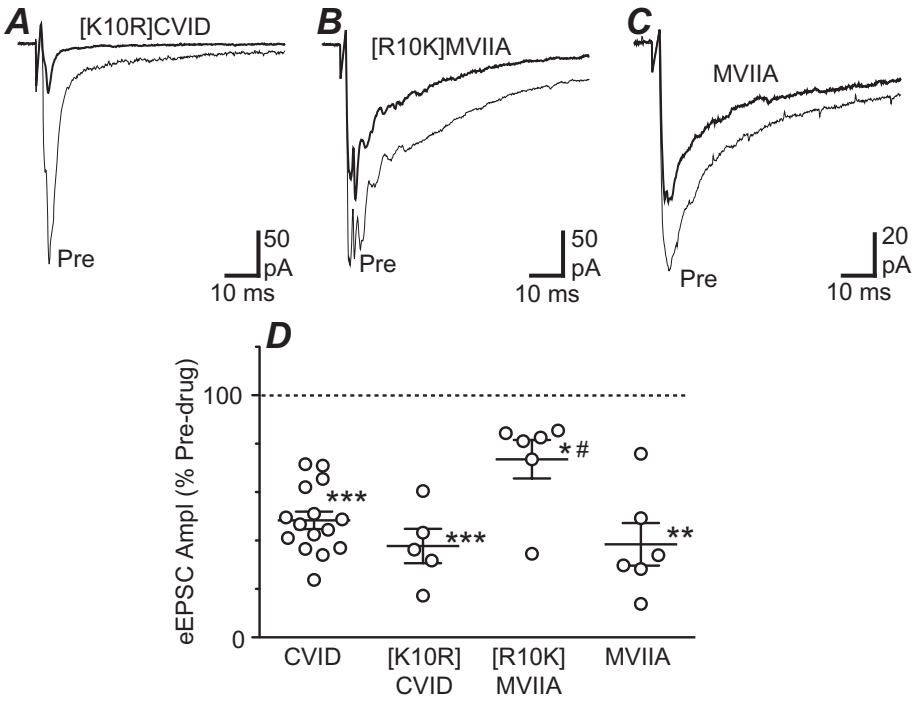

Figure 4

Conotoxins inhibit evoked EPSCs in superficial dorsal horn. Averaged traces of evoked EPSCs before (pre) and during application of 100 nM (A) [K10R]CVID, (B) [R10K]MVIIA and (C) MVIIA. (D) Scatter plots of the reduction in evoked EPSCs produced by the conotoxins, shown as the evoked EPSC amplitude in the presence of conotoxin as a percentage of the pre-conotoxin value. In (D) lines show mean ± SEM; *, ** and *** $P < 0.05$, 0.01, 0.001 (drug vs. pre-drug) and # $P < 0.05$ ([R10K]MVIIA versus CVID, [K10R]CVID and MVIIA).

highest doses tested (Scott *et al.*, 2002; Smith *et al.*, 2002). We measured the TI of CVID and MVIIA as the ratio of their ED_{50}s for anti-allodynia versus side-effect induction. The TI for CVID and MVIIA was 1.8 and 1.0, respectively, when comparing rotarod performance, and was 2.4 and 0.7, respectively, when comparing the visually scored behaviours. The present results differ from a previous study in which CVID (9.7) had a greater TI than MVIIA (2.1) in a neuropathic model (Scott *et al.*, 2002). The difference between these studies might be due to the use of different neuropathic pain models (partial sciatic nerve ligation vs. tight spinal nerve ligation). It might be noted that a relatively high TI has also been observed for intrathecal CVID in an animal model of inflammation (Smith *et al.*, 2002). The difference might also be due to the additional assessment of motor incoordination with the rotarod test in the present study. Indeed, CVID had only a 1.7× greater TI than MVIIA when using the rotarod test as a side-effect measure. By comparison, our study and that by Scott *et al.* (2002) found that CVID had a 3.7× and a 4.6× greater TI than MVIIA, respectively, when using the visual scoring system. This suggests that the rotarod provides a more sensitive side-effect measure than the visual scoring system, at least for conotoxins, and that a range of side effects should be examined when assessing the TI of analgesics.

In order to determine the mechanism underlying the differences between the functional analgesic properties of these conotoxins, we examined their effect on primary afferent evoked synaptic transmission in a spinal pain pathway. Potential differences between the conotoxins include their selectivity, potency, efficacy or site of action. In the present study, it was found that CVID and MVIIA both reduced non-NMDA-mediated synaptic transmission into lamina II of the superficial dorsal horn similar to that observed previously for the $Ca_v2.2$ selective conotoxins CVID, GVIA and MVIIA (Heinke *et al.*, 2004; Rycroft *et al.*, 2007; Motin and Adams, 2008). The inhibition of synaptic transmission was likely to be mediated by presynaptic inhibition of neurotransmitter release from primary afferent nociceptor terminals within the dorsal horn. First, EPSC were evoked by focal stimulation of the dorsal roots that contain primary afferent fibres, as in other studies (Heinke *et al.*, 2004; Rycroft *et al.*, 2007; Motin and Adams, 2008). Second, the CVID- and MVIIA-induced inhibition of evoked EPSCs was associated with an increase in the paired pulse ratio of closely evoked EPSCs, which is indicative of a presynaptic site of action and consistent with prior observations on Sr^{2+}-evoked asynchronous EPSCs (Rycroft *et al.*, 2007). In the current study, CVID had an EC_{50} of 69 nM that is similar to its potency at $Ca_v2.2$ VGCCs in isolated dorsal root ganglion neurons and cell lines (Motin *et al.*, 2007; Murali *et al.*, 2012). While the maximal inhibition of evoked EPSCs was similar to that observed in some studies using $Ca_v2.2$ selective ω-conotoxins (Heinke *et al.*, 2004; Rycroft *et al.*, 2007), it was less than the complete inhibition observed previously (Motin and Adams, 2008). This difference might have been due to differences in the temperature of recordings. It may have also been due to differences in age because the present *in vitro* experiments were carried out in 2- to 3-week-old rats (compared with less

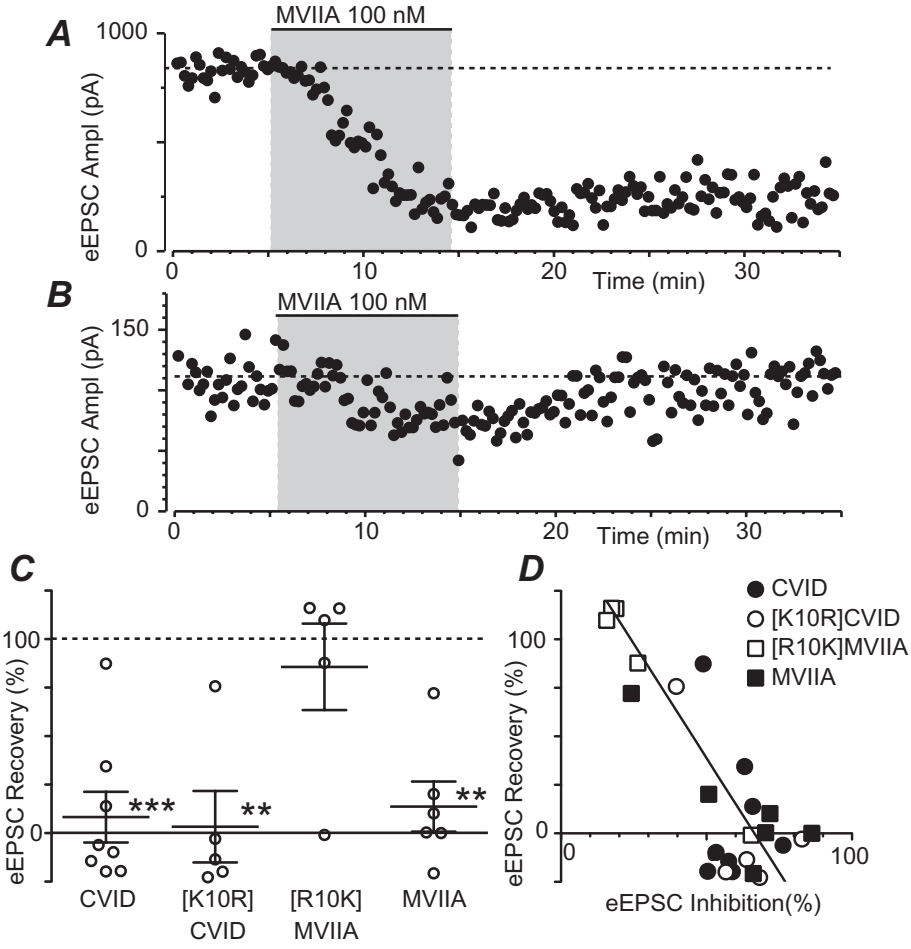

Figure 5

Recovery from conotoxin inhibition is dependent upon the degree of inhibition. (A,B) Time plots of the amplitude of dorsal root evoked EPSCs in two different lamina II neurons during superfusion of 100 nM MVIIA (shaded area), with recovery during 20 min of washout. (C) Scatter plots of the recovery of evoked EPSC amplitude following washout of CVID, [K10R]CVID, [R10K]MVIIA and MVIIA; data shown as the evoked EPSC amplitude at 20 min post-wash as a percentage of the pre-conotoxin application value. (D) Plot of the recovery of evoked EPSC amplitude following 20 min wash (eEPSC wash) versus the inhibition of evoked EPSC amplitude during conotoxin application (eEPSC drug); both values expressed as a percentage of the pre-conotoxin application value. In (C), lines show mean ± SEM; *, ** and *** $P < 0.05$, 0.01, 0.001 (wash vs. pre-drug). In (D), the linear best-fit line to all conotoxins is shown.

than 2 weeks old in Motin and Adams, 2008), and there are developmental changes in spinal VGCC expression during the first two post-natal weeks (Iwasaki *et al.*, 2000).

It has been suggested that differences in ligand unbinding from VGCCs impacts upon the analgesic utility of different conotoxins (Wright *et al.*, 2000; Adams *et al.*, 2012). The inhibition of VGCC currents in isolated neurons produced by CVID is much more reversible after washout than MVIIA and that this is due largely to the basic amino acid residue at position 10 of the peptide sequence (Mould *et al.*, 2004). This residue is an arginine in MVIIA and a lysine in CVID. Indeed, mutation of residue 10 to arginine in CVID to [K10R]CVID impairs the reversibility of VGCC inhibition, while mutation to lysine in MVIIA to [R10K]MVIIA increases it (Mould *et al.*, 2004).

We observed that the time course of anti-allodynia was not solely dependent upon the type of amino acid at residue 10. While the conotoxins produced similar maximal anti-allodynic effects, CVID and [K10R]CVID had a quicker reversal of anti-allodynia following washout than MVIIA and [R10K]MVIIA. The time course of motor disruption produced by the conotoxins also mirrored the time course of anti-allodynia produced by these agents, with MVIIA having a longer duration of action. [K10R]CVID and [R10K]MVIIA had a lesser effect on rotarod performance compared with CVID and MVIIA, although they produced similar side effects to CVID and MVIIA when using the visual scoring system. It is therefore possible that the hybrid conotoxins could provide a potential therapeutic alternative to CVID and MVIIA that is independent of the type of amino acid at residue 10.

We also observed a lack of correlation between the position 10 residue and recovery from inhibition at the cellular level. In spinal cord slices, the inhibition of evoked EPSCs produced by [K10R]CVID and [R10K]MVIIA was variable, as was the recovery of evoked EPSCs following washout of CVID, MVIIA, [K10R]CVID and [R10K]MVIIA. This variability

in recovery was dependent upon the degree of inhibition but was independent of the conotoxin type. This differs to the findings for VGCC inhibition in isolated neurons where recovery is dependent upon both the degree of inhibition and the conotoxin type (Mould *et al.*, 2004).

Together, the present experiments indicate that the *in vitro* actions of conotoxins in the spinal cord slice preparation and their *in vivo* effects following intrathecal delivery are largely determined by factors other than the residue at position 10. Ligand-induced inhibition and unbinding from VGCCs are influenced by the state of depolarization (Lewis *et al.*, 2012), and unlike the experimental conditions used to study VGCCs in isolated neurons, presynaptic terminals in spinal cord slices and in whole animals are not held under voltage clamp conditions. The actions of conotoxins are also influenced by VGCCs auxiliary subunits (Mould *et al.*, 2004; Lewis *et al.*, 2012), and these are altered in neuropathic pain models (Li *et al.*, 2004; Boroujerdi *et al.*, 2008). In this regard, the cellular actions of conotoxins in the present and prior slice studies have been carried out using tissue from naïve animals. While there are no conotoxins studies using slices from neuropathic animals, it might be noted than CVID inhibition of evoked EPSCs is reduced in an inflammatory pain model (Rycroft *et al.*, 2007). Finally, the actions of conotoxins are likely to be limited by their distribution and metabolism. In this regard, the conotoxins are likely to have relatively poor access to binding sites within presynaptic terminals in whole animals and the slice preparation compared with isolated neurons, which could provide a rate limiting step in their reversibility.

In summary, the present study indicates that the conotoxins CVID and MVIIA both reduce the mechanical allodynia associated with an animal model of neuropathic pain. Unlike prior studies, the current results suggest that CVID has only a marginally better greater TI that MVIIA. Two intermediate hybrids, [K10R]CVID and [R10K]MVIIA, displayed lesser disruption of motor performance; however, they still displayed other side effects. CVID, MVIIA and the hybrids inhibited primary afferent evoked synaptic transmission into the superficial dorsal horn in a similar manner. Alteration of residues in these conotoxins might therefore present an alternative approach to improving the TI of these analgesic agents.

Acknowledgements

This work was supported by grants from the National Health & Medical Research Council Program Grant (569927 to RJL and MJC) and Senior Principal Research Fellowship (511914 to MJC).

Conflicts of interest

The authors declare no conflicts of interest.

References

Adams DJ, Smith AB, Schroeder CI, Yasuda T, Lewis RJ (2003). Omega-conotoxin CVID inhibits a pharmacologically distinct voltage-sensitive calcium channel associated with transmitter release from preganglionic nerve terminals. J Biol Chem 278: 4057–4062.

Adams DJ, Callaghan B, Berecki G (2012). Analgesic conotoxins: block and G protein-coupled receptor modulation of N-type (Ca(V) 2.2) calcium channels. Br J Pharmacol 166: 486–500.

Alexander SPH, Mathie A, Peters JA (2011). Guide to receptors and channels (GRAC), 5th edition. Br J Pharmacol 164 (Suppl. 1): S1–S324.

Berecki G, Motin L, Haythornthwaite A, Vink S, Bansal P, Drinkwater R *et al.* (2010). Analgesic (omega)-conotoxins CVIE and CVIF selectively and voltage-dependently block recombinant and native N-type calcium channels. Mol Pharmacol 77: 139–148.

Berry MS, Pentreath VW (1976). Criteria for distinguishing between monosynaptic and polysynaptic transmission. Brain Res 105: 1–20.

Blake DW, Scott DA, Angus JA, Wright CE (2005). Synergy between intrathecal omega-conotoxin CVID and dexmedetomidine to attenuate mechanical hypersensitivity in the rat. Eur J Pharmacol 506: 221–227.

Boroujerdi A, Kim HK, Lyu YS, Kim DS, Figueroa KW, Chung JM *et al.* (2008). Injury discharges regulate calcium channel alpha-2-delta-1 subunit upregulation in the dorsal horn that contributes to initiation of neuropathic pain. Pain 139: 358–366.

Bowersox SS, Gadbois T, Singh T, Pettus M, Wang YX, Luther RR (1996). Selective N-type neuronal voltage-sensitive calcium channel blocker, SNX-111, produces spinal antinociception in rat models of acute, persistent and neuropathic pain. J Pharmacol Exp Ther 279: 1243–1249.

Chaplan SR, Pogrel JW, Yaksh TL (1994). Role of voltage-dependent calcium channel subtypes in experimental tactile allodynia. J Pharmacol Exp Ther 269: 1117–1123.

Dworkin RH, O'Connor AB, Audette J, Baron R, Gourlay GK, Haanpaa ML *et al.* (2010). Recommendations for the pharmacological management of neuropathic pain: an overview and literature update. Mayo Clin Proc 85: S3–S14.

Ekberg J, Jayamanne A, Vaughan CW, Aslan S, Thomas L, Mould J *et al.* (2006). muO-conotoxin MrVIB selectively blocks Nav1.8 sensory neuron specific sodium channels and chronic pain behavior without motor deficits. Proc Natl Acad Sci U S A 103: 17030–17035.

Hama A, Sagen J (2009). Antinociceptive effects of the marine snail peptides conantokin-G and conotoxin MVIIA alone and in combination in rat models of pain. Neuropharmacology 56: 556–563.

Heinke B, Balzer E, Sandkuhler J (2004). Pre- and postsynaptic contributions of voltage-dependent Ca2+ channels to nociceptive transmission in rat spinal lamina I neurons. Eur J Neurosci 19: 103–111.

Iwasaki S, Momiyama A, Uchitel OD, Takahashi T (2000). Developmental changes in calcium channel types mediating central synaptic transmission. J Neurosci 20: 59–65.

Jensen TS, Baron R, Haanpaa M, Kalso E, Loeser JD, Rice AS *et al.* (2011). A new definition of neuropathic pain. Pain 152: 2204–2205.

Jeong HJ, Vandenberg RJ, Vaughan CW (2010). N-arachidonyl-glycine modulates synaptic transmission in superficial dorsal horn. Br J Pharmacol 161: 925–935.

Lewis RJ, Nielsen KJ, Craik DJ, Loughnan ML, Adams DA, Sharpe IA *et al.* (2000). Novel omega-conotoxins from Conus catus discriminate among neuronal calcium channel subtypes. J Biol Chem 275: 35335–35344.

Lewis RJ, Dutertre S, Vetter I, Christie MJ (2012). Conus venom peptide pharmacology. Pharmacol Rev 64: 259–298.

Li CY, Song YH, Higuera ES, Luo ZD (2004). Spinal dorsal horn calcium channel alpha2delta-1 subunit upregulation contributes to peripheral nerve injury-induced tactile allodynia. J Neurosci 24: 8494–8499.

McGivern JG (2006). Targeting N-type and T-type calcium channels for the treatment of pain. Drug Discov Today 11: 245–253.

Malmberg AB, Yaksh TL (1995). Effect of continuous intrathecal infusion of omega-conopeptides, N-type calcium-channel blockers, on behavior and antinociception in the formalin and hot-plate tests in rats. Pain 60: 83–90.

Morimoto S, Ito M, Oda S, Sugiyama A, Kuroda M, Adachi-Akahane S (2012). Spinal mechanism underlying the antiallodynic effect of gabapentin studied in the mouse spinal nerve ligation model. J Pharmacol Sci 118: 455–466.

Motin L, Adams DJ (2008). omega-Conotoxin inhibition of excitatory synaptic transmission evoked by dorsal root stimulation in rat superficial dorsal horn. Neuropharmacology 55: 860–864.

Motin L, Yasuda T, Schroeder CI, Lewis RJ, Adams DJ (2007). Omega-conotoxin CVIB differentially inhibits native and recombinant N- and P/Q-type calcium channels. Eur J Neurosci 25: 435–444.

Mould J, Yasuda T, Schroeder CI, Beedle AM, Doering CJ, Zamponi GW *et al*. (2004). The alpha2delta auxiliary subunit reduces affinity of omega-conotoxins for recombinant N-type (Cav2.2) calcium channels. J Biol Chem 279: 34705–34714.

Murali SS, Napier IA, Rycroft BK, Christie MJ (2012). Opioid-related (ORL1) receptors are enriched in a subpopulation of sensory neurons and prolonged activation produces no functional loss of surface N-type calcium channels. J Physiol (Lond) 590: 1655–1667.

Ogawa K, Takasu K, Shinohara S, Yoneda Y, Kato A (2011). Pharmacological characterization of lysophosphatidic acid-induced pain with clinically relevant neuropathic pain drugs. Eur J Pain 16: 994–1004.

Rycroft BK, Vikman KS, Christie MJ (2007). Inflammation reduces the contribution of N-type calcium channels to primary afferent synaptic transmission onto NK1 receptor-positive lamina I neurons in the rat dorsal horn. J Physiol (Lond) 580: 883–894.

Scott DA, Wright CE, Angus JA (2002). Actions of intrathecal omega-conotoxins CVID, GVIA, MVIIA, and morphine in acute and neuropathic pain in the rat. Eur J Pharmacol 451: 279–286.

Seltzer Z, Dubner R, Shir Y (1990). A novel behavioral model of neuropathic pain disorders produced in rats by partial sciatic nerve injury. Pain 43: 205–218.

Smith MT, Cabot PJ, Ross FB, Robertson AD, Lewis RJ (2002). The novel N-type calcium channel blocker, AM336, produces potent dose-dependent antinociception after intrathecal dosing in rats and inhibits substance P release in rat spinal cord slices. Pain 96: 119–127.

Snutch TP (2005). Targeting chronic and neuropathic pain: the N-type calcium channel comes of age. NeuroRx 2: 662–670.

Souza AH, Ferreira J, Cordeiro Mdo N, Vieira LB, De Castro CJ, Trevisan G *et al*. (2008). Analgesic effect in rodents of native and recombinant Ph alpha 1beta toxin, a high-voltage-activated calcium channel blocker isolated from armed spider venom. Pain 140: 115–126.

Vuong LAQ, Mitchell VA, Vaughan CW (2008). Actions of N-arachidonyl-glycine in a rat neuropathic pain model. Neuropharmacology 54: 189–193.

Westenbroek RE, Hell JW, Warner C, Dubel SJ, Snutch TP, Catterall WA (1992). Biochemical properties and subcellular distribution of an N-type calcium channel alpha 1 subunit. Neuron 9: 1099–1115.

Wright CE, Robertson AD, Whorlow SL, Angus JA (2000). Cardiovascular and autonomic effects of omega-conotoxins MVIIA and CVID in conscious rabbits and isolated tissue assays. Br J Pharmacol 131: 1325–1336.

Yamamoto T, Sakashita Y (1998). Differential effects of intrathecally administered N- and P-type voltage-sensitive calcium channel blockers upon two models of experimental mononeuropathy in the rat. Brain Res 794: 329–332.